10.3389/fmars.2023.1135113

the East China Sea, and the South China Sea into the Northwest Pacific were 29~32 t/y, 159~302 t/y, 142~616 t/y, and -298~34 t/y, respectively. This study highlights the importance of considering the cross-shelf REE fluxes in the Northwest Pacific when constructing the oceanic REE budgets.

KEYWORDS

Northwest Pacific, rare earth elements, remineralization, water mass tracing, cross-shelf fluxes

1 Introduction

The Northwest Pacific, which mainly includes the Northwest Pacific subarctic region and the Northwest Pacific subtropical region, is adjacent to a large area of marginal seas and is a key area that receives trace element inputs from terrigenous sources (Nishioka et al., 2013 ; Kim et al., 2017; Yang et al., 2018; Morton et al., 2019). The Kuroshio (including Kuroshio Extension) and Oyashio are the two most important surface currents in the Northwest Pacific. They carry large quantities of trace elements (Fe/Mn/Cd/Zn, etc.) from the marginal seas (Sea of Okhotsk and East China Sea, etc.) and islands (Kuril and Aleutian Islands, etc.) into the Northwest Pacific (Nishioka et al., 2013 ; Kim et al., 2017; Yang et al., 2018; Morton et al., 2019). Rare earth elements (REEs, the lanthanide family) are important marine process tracers with coherent chemical properties and similar chemical behaviors (Elderfield, 1988). They are commonly used to trace lithogenic input sources and water mixing , which are in turn very important for understanding the behavior of trace elements in the oceans (Zhang et al., 2008; Zheng et al., 2016; Behrens et al., 2018a; Garcia-Solsona et al., 2020; Behrens et al., 2020). For instance, La/Yb ratios (the ratio of La to Yb after normalization) reflected the recent dissolution of lithogenic material from the Kerguelen and/or Heard islands in the Southern Ocean (Zhang et al., 2008). The REE anomaly (the anomaly refers to the deviation of the measured value of one element to the value predicted from two adjacent elements after normalization) in the Northwest Pacific was used to trace inputs from the Philippine Islands (Behrens et al., 2018a). In addition, heavy rare earth elements (HREEs; Gd, Td, Dy, Ho, Er, Tm, Yb, Lu), which generally behave conservatively, have been utilized to identify water mass mixing (Zhang et al., 2018; Garcia-Solsona et al., 2020; Liu et al., 2022).

The concentrations of REEs in the ocean generally increase with depth, which can be explained by the scavenging of REEs at the surface and the release of REEs by remineralization at depth (Elderfield and Greaves, 1982; de Baar et al., 1985; Elderfield, 1988; Bertram and Elderfield, 1993). Numerous studies have investigated the effect of organic matter remineralization on REEs using the relationship between REEs and apparent oxygen utilization (AOU; a reliable measure of remineralization) (e.g., Stichel et al., 2015; Lambelet et al., 2016; Behrens et al., 2018b; Seo and Kim, 2020). For example, in the eastern Atlantic, organic matter remineralization releases more Nd than in the western Atlantic (Stichel et al., 2015; Lambelet et al., 2016). However, at present, REE data is sparse in the Northwest Pacific (Piepgras and Jacobsen, 1992; Alibo and Nozaki, 1999; Behrens et al., 2018a), and thus our knowledge of the regional differences in the effects of remineralization on REEs is limited.

The mass balance of dissolved REEs in the oceans is not well constrained (Tachikawa et al., 2003; Johannesson and Burdige, 2007). Marginal seas may be a major source of material to the open oceans, and typically have high concentrations of REEs due to excessive inputs from the atmosphere, rivers, groundwater, and land-sea boundary exchanges (Amakawa et al., 2004a; Amakawa et al., 2004b; Hatta and Zhang, 2006; Wu et al., 2015; Zhang et al., 2018). The Northwest Pacific Ocean interacts with a large continental shelf area (~6.10 ^{6} km^{2}), which accounts for about 20 % of the total area of global marginal seas. Therefore, marginal seas may play a key role in the supply and mass balance of REEs throughout the Pacific. However, quantitative evaluations of cross-shelf fluxes of REEs from marginal seas to the open ocean are lacking. The influence of marginal seas on oceanic REE budgets is still poorly understood.

To better understand the influencing factors and sources of REEs in the Northwest Pacific, we measured the dissolved REEs in seawater above 2000 m in the region from 13°N to 40°N along a 150°E longitudinal transect. We found regional differences in the release of REEs by organic matter remineralization. In addition, we identified the sources of REEs and suggest that REE ratios can be good tracers of water masses originating from the subarctic region. Furthermore, we estimated the cross-shelf fluxes of REEs between the marginal seas and the Northwest Pacific. Our results indicate that the marginal seas have a very important role in the REE budgets of the Northwest Pacific.

2 Materials and methods

2.1 Study area

The Northwest Pacific, from the subarctic to the subtropical region, interacts with the Sea of Okhotsk, Sea of Japan, East China Sea, South China Sea, and the Bering Sea.

The Kuroshio Current and Oyashio Current are the most important currents in the Northwest Pacific (Figure 1). The Kuroshio originates from the western boundary current to the east

FIGURE 1
Map of stations sampled during the transect P1 cruise (blue dots) in the northwest Pacific, and generalized circulation patterns in the region. Solid arrows represent flow patterns of major surface currents (the North Equatorial Current, the Kuroshio Current, the Oyashio Current, the East Kamchatka Current). The map was created using Ocean Data View (ODV) software (Schlitzer, 2015).

of the Philippine Islands, and is characterized by high temperature, high salinity oligotrophic water (Nitani, 1972). It flows northward along Taiwan Island, passes through the East China Sea continental shelf, then flows into the Pacific Ocean through the Tokara Strait, and turns eastward at about 35°N. The Oyashio is formed by mixing of the East Kamchatka Current and Okhotsk water, which is characterized by low temperature and low salinity water, rich in oxygen and nutrients (Rogachev et al., 2000). As the Oyashio front intrudes southward, it interacts with warm and saline Kuroshio waters to form North Pacific Intermediate Water (NPIW). This region is defined as the Mixed Water Region (MWR) (stations P1-1~P1-4; Talley et al., 1995; Yasuda et al., 1996; Yasuda, 2004; Qiu and Chen, 2011; Hu et al., 2015).

At stations P1-7~P1-28 (Figure 1), North Pacific Tropical Water (NPTW) is the dominant North Pacific subsurface water mass, and is characterized by a salinity maximum (S>34.60, Suga et al., 2000). NPIW is formed in the MWR and flows cyclonically in the North Pacific. It is usually defined by a potential density of 26.6-27.5 kg/m^3 and features a vertical salinity minimum in the subtropical Pacific (Yasuda et al., 2001; Nishioka et al., 2007; Kim et al., 2017).

2.2 Sample collection and ancillary data

Seawater samples shallower than 2000 m were collected along a longitudinal transect P1 (13°N ~ 40°N, 150°E) during a cruise on the R/V Dongfanghong 3 (October 31st to December 1st, 2019) in the Northwest Pacific. The stations are shown in Figure 1. Stations P1-1~P1-4 are located in the MWR and stations P1-7~P1-28 are located in the subtropical region.

Seawater was sampled from 12 L Niskin-X bottles and filtered immediately through 0.45 μm membrane filters (polyether sulfone) into pre-cleaned low-density polyethylene (LDPE) bottles (500 mL). The filtering process was conducted in a clean bench onboard. Samples were then acidified to pH≤ 2 using 6 M ultra-pure hydrochloric acid (Optima grade, Fisher Chemical), and stored in double bags.

Water temperature and salinity profiles were measured using conductivity-temperature-depth sensors (CTD, Sea-Bird 911 plus). The dissolved oxygen (DO) concentration was determined via Winkler titration (Bryan et al., 1976). AOU was calculated by the equation below,

$$AOU = DO^s - DO \quad (1)$$

where, DO^s and DO represent the saturated oxygen concentration at the given pressure/depth and the observed oxygen concentration, respectively. Chlorophyll was measured using a HITACHI F-4700 fluorometer (Parsons et al., 1984; Li et al., 2022). Nitrate and nitrite concentrations were measured using an autoanalyzer (Seal analytical AA3) (Li et al., 2022).

2.3 Rare earth element analysis

Seawater samples were pre-concentrated with NOBIAS PA1 resin in a Class 1000 clean room and the REE concentrations were determined by inductively coupled plasma mass spectrometry (ICP-MS; Takata et al., 2009; Persson et al., 2011; Hatje et al., 2014; Liu et al., 2022). The results were corrected using a Lu (lutecium) internal standard. The recoveries of the internal standard were greater than 90%. The concentration of REEs in blank samples was within 3% of that measured in surface seawater, which usually has the lowest concentration in the ocean. Relative standard deviations (RSDs) of REEs were determined on replicate measurements of

surface (n=4) and 4000 m deep (n=11) seawater, which were both less than 5%. The sample measurement errors are reported in Supplementary Table S1.

The Ce anomaly (Ce/Ce*) was calculated as (Zhang and Nozaki, 1998; Lacan and Jeandel, 2001):

$$Ce/Ce^{*} = 2 \times (Ce)_N/((La)_N + (Pr)_N) \quad (2)$$

where $(Ce)_N$, $(La)_N$,and $(Pr)_N$ represent the Post Archean Australian Shale (PAAS) (Taylor and McLennan, 1985) normalized Ce, La, and Pr, respectively. The RSD of Ce/Ce* in Pacific deep water (4000 m, n=11) is 3.5%. By convention, an anomaly value >1 (or <1) is referred to as a positive (or negative) anomaly.

The La/Yb ratio was calculated as (Zhang et al., 2008):

$$La/Yb = (La)_N/(Yb)_N \quad (3)$$

where $(Yb)_N$ represents the PAAS normalized Yb. The RSD of the La/Yb ratio in Pacific deep water is 2.4% (4000 m, n=11).

The location of station P1-15 (26°N, 150°E) in this study is close to station TPS 24 271-1 (24.29°N, 150.45°E) from previous trans-Pacific sections (Piepgras and Jacobsen, 1992). The REE concentrations were comparable between the two stations (1000 m and 2000 m) with RSDs <10 % except for Ce (Supplementary Table S2). Considering that Ce is susceptible to contamination and has a relationship with latitude (see section 4.2), the Ce concentration RSDs of 18 % and 19 % are acceptable. The intercalibration reported here basically follows GEOTRACES protocols (https://geotracesold.sedoo.fr/Cookbook.pdf).

2.4 Isopycnal mixing model

To evaluate the quasi-conservative behavior of REEs from NPIW (26.6~27.5 kg/m^3) in the MWR (stations P1-1~P1-4), we used a mixing model to determine the Oyashio and Kuroshio mixing ratios at three isopycnal surfaces: 26.6, 27.0 and, 27.5 kg/m^3 (Du et al., 2013; Wu et al., 2015; Li et al., 2021). The equations are as follows:

$$f_{OC} + f_{KC} = 1 \quad (4)$$

$$f_{OC} \times q_{OC} + f_{KC} \times q_{KC} = q_M \quad (5)$$

$$f_{OC} \times S_{OC} + f_{KC} \times S_{KC} = S_M \quad (6)$$

$$DNd = Nd_M - f_{OC} \times Nd_{OC} - f_{KC} \times Nd_{KC} \quad (7)$$

where, f_{OC} and f_{KC} represent the fractions of the Oyashio and the Kuroshio waters, respectively, and the q_{OC} (q_{KC}), S_{OC}(S_{KC}),and Nd_{OC}(Nd_{KC}) terms are the potential temperatures (q), salinities, and Nd concentrations of Oyashio (Kuroshio) end-members, respectively. We selected stations located in regions before the end-member currents enter the MWR since water mass properties may change after formation during transport to the study area. End-member characteristics of the Oyashio and the Kuroshio and their uncertainties are listed in Table 1. The subscript "M" represents measured values. Calculated results were fitted by least-squares optimization. Non-conservative Nd (DNd) is defined as the difference between the observed concentrations and calculated values due to water mass mixing; DNd values greater than 0 or less than 0 represent additions or removals from our defined endmember region to the study region, respectively.

3 Results

3.1 Hydrographic setting

The potential temperature-salinity diagram (Figure 2) shows a potential temperature range from 1.7 to 29.5°C. At low latitudes, the surface water (≤5 m) has higher potential temperatures than that at high latitudes (Figure 3A). Potential temperature in surface water at stations P1-1~P1-4 (MWR, 37°N-40°N) ranges from 14.5 to 22.3°C. At stations P1-7~P1-28 (subtropical region, 13°N-34°N), the potential temperature in surface water ranges from 22.3 to 29.4°C. Vertically, the potential temperature decreases rapidly to <5°C from the surface to 1000 m and then remains constant below 1000 m (Figure 3A).

TABLE 1 End-member characteristics of the Oyashio and the Kuroshio currents and their uncertainties.

Water mass	Oyashio			Kuroshio		
Potential density (kg/m^3)	26.6	27	27.5	26.6	27	27.5
q (°C)	2.18±0.16 (n=15)[a]	2.95±0.22 (n=14)[a]	2.78±0.15 (n=13)[a]	8.26±0.45 (n=10)[b]	5.03±0.46 (n=10) [b]	3.14±0.13 (n=9)[b]
Salinity	33.31±0.14 (n=15)[a]	33.88±0.03 (n=14)[a]	34.34±0.01 (n=13)[a]	34.19±0.09 (n=10)[b]	34.14±0.07 (n=10)[b]	34.40±0.02 (n=9)[b]
Location	40.0°~43°N 145°~153°E	40.0°~43°N 146°~153°E	40.0°~43°N 146°~153°E	32°~35°N 142°~146°E	32°~35°N 142°~146°E	32°~34°N 142°~146°E
Nd (pmol/kg)	17.50 (n=1)[c]	20.10 (n=1)[c]	23.00 (n=1)[c]	10.29 (n=1)[d]	14.41 (n=1)[d]	18.40 (n=1)[d]
Location	40.5°N, 144.5°E			34.7°N, 139.9°E		

[a]Mean values from the P01 transect (stations 2-30) with potential densities of 26.6, 27, and 27.5 kg/m^3 (WOCE dataset, http://www.ewoce.org).
[b]Mean values from the P10 transect (stations 79-86) and PR3N (stations 6021 and 6023) with potential densities of 26.6, 27, and 27.5 kg/m^3 (WOCE dataset, http://www.ewoce.org).
[c]Amakawa et al., 2004a.
[d]Alibo and Nozaki, 1999.

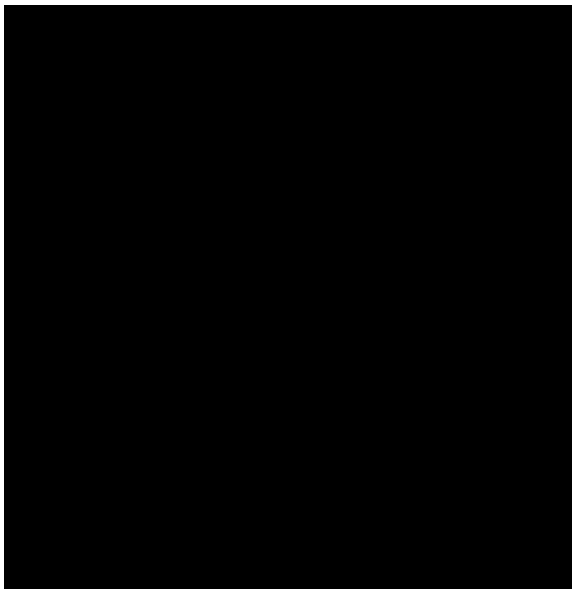

FIGURE 2
Potential temperature (℃)-salinity diagram with potential density (kg/m ^{3}) contours as solid grey lines. The general location of major currents (Oyashio and Kuroshio) and water masses (NPTW: North Pacific Tropical Water, NPIW: North Pacific Intermediate Water) are marked based on their hydrographic properties. Colored symbols represent the Nd concentration (pmol/kg) of individual water samples. The shallow water (<100 m) in MWR was marked by a dotted ellipse.

Salinity ranges from 33.39 to 35.12. In the upper water column (≤300 m), stations P1-1 ~P1-4 have low salinities, 33.39 to 34.55, which is mainly influenced by the Oyashio. In contrast, the other stations have high salinities (34.12 to 35.12), where the NPTW forms (Figure 3B). Below 300 m, the salinities at stations P1-1 and P1-2 gradually increase with depth. However, the salinities of the other stations reach their minimum values (<34.3) between 300 m and 1000 m, which indicates the core area of NPIW (26.6-27.5 kg/m^3, Figures 3B, 4A). The salinities at all stations are constant at 34.20-34.63 in deeper water (1000 m-2000 m).

FIGURE 3
Distributions of (A) potential temperature (℃), (B) salinity with potential density contours in white, (C) DO (㎜ol/kg), (D) Nd (pmol/kg), (E) Yb (pmol/kg), and (F) Ce (pmol/kg) along the P1 transect.

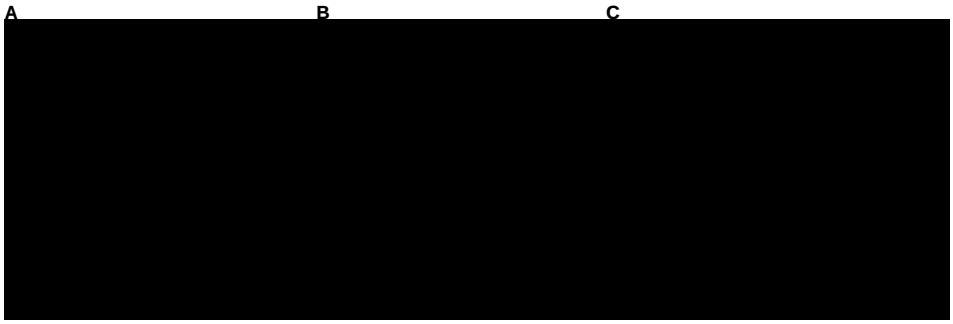

FIGURE 4
Vertical profiles of (A) Salinity, (B) Nd (pmol/kg), and (C) Yb (pmol/kg) with error bars from all stations.

3.2 REEs concentrations

Detailed REE concentration data is shown in Supplementary Table S1. Similar distributions were observed for Nd and the sum of LREEs (Light rare earth elements ; La , Ce, Pr, Nd, Sm, and Eu; except for Ce, which has significant redox-related behavior that other LREEs do not; R^2=0.98), and Yb and the sum of HREEs (R^2=0.98) (Supplementary Figures S1,S2), Therefore, we use Nd as a representative element for LREEs and Yb as a representative element for the HREEs (e.g., Zheng et al., 2016; de Baar et al., 2018) in this study.

The concentrations of Nd and Yb for all stations along the P1 transect are shown in Figures 3D, E. Concentrations of Nd and Yb ranged from 2.62 ~ 26.66 pmol/kg and 0.83 ~ 10.02 pmol/kg, respectively. In general, REE concentrations in the MWR were higher than those in the subtropical region. In the MWR (37-40°N, stations P1-1~P1-4), the water samples from less than 300 m depth (<26.6 kg/m^3) were characterized by high REE concentrations (Nd=13.02±2.91 pmol/kg, Yb=3.60±1.03 pmol/kg), which may indicate significant influence by the Oyashio with low salinity and high REEs. Below 300 m, the REEs increased with depth (Figures 3D, E, 4B, C). At 2000 m, the concentrations of Nd and Yb were 22.70 ±2.39 pmol/kg and 9.68±2.91 pmol/kg, respectively. In the subtropical region (13-34°N, stations P1-7~P1-28), the lowest REEs concentrations were found in surface and subsurface water (≤105 m, Nd=4.45±1.20 pmol/kg, Yb=1.18±0.26 pmol/kg), which may be due to particle scavenging (Stichel et al., 2015; Frie et al., 2016). Below 105 m, the REE concentrations increased with depth (Figures 3D, E, 4B, C). At 2000 m, the concentrations of Nd and Yb reached up to 21.44±2.92 pmol/kg and 9.04±0.68 pmol/kg, respectively.

Due to its significant redox behavior, Ce concentration distributions differed from other REEs (Figure 3F). The highest Ce concentration (6.29±1.94 pmol/kg) was found at a water depth less than 300 m in the MWR. The lowest Ce concentration was found in water samples from 500 m to 2000 m depths at stations P1-19~P1-28 (1.77±0.22 pmol/kg). Overall, at the same depth, Ce concentrations were higher at high latitudes than at low latitudes (except for ~1500 m at stations P1-7~P1-9). At ~1500 m of stations P1-7~P1-9, Ce concentrations (5.49 ±1.12 pmol/kg, Figure 3F) were slightly higher than the surrounding seawater and the oxygen was the lowest (46.69±1.50 μmol/kg, Figure 3C) as well.

4 Discussion

4.1 Processes controlling the vertical distributions of REEs: remineralization

REE concentrations were strongly positively correlated with AOU below the depth of the chlorophyll maximum (DCM) layer (Figure 5A, the DCM in each station is shown in Supplementary Table S1), suggesting that the remineralization of sinking organic

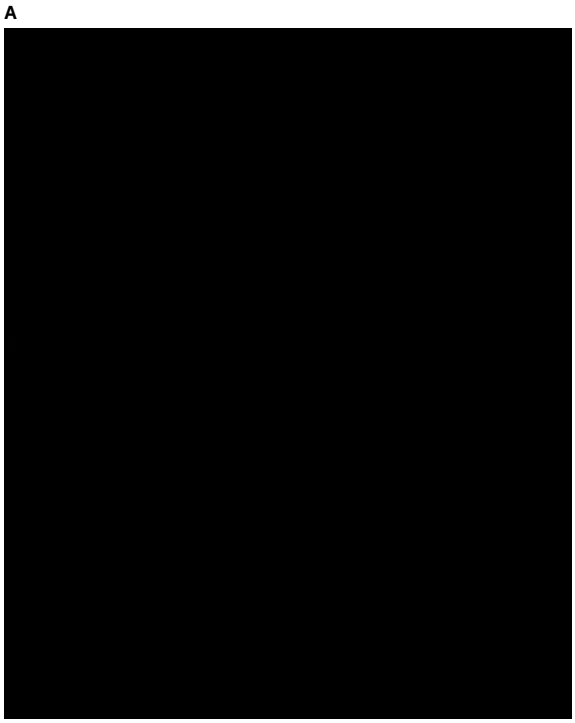

FIGURE 5
(A) Nd (pmol/kg) vs. AOU (μmol/kg) from P1 transect (triangles) and Behrens et al. (2018a,b) (crosses) within subsurface and intermediate water (Depth >DCM and s_q< 27.5 kg/m^3); (B) Nd (pmol/kg) vs. Nitrate +Nitrite (μmol/kg) from P1 transect (triangles). The colored symbols represent data from water less dense than 26.6 kg/m^3 in the MWR (stations P1-1~P1-4, 37~40°N). The linear regressions and corresponding equations are shown for water samples with densities less than 26.6 kg/m^3 in the MWR (blue line) and south of the MWR (gray line).

matter contributes to the increase of REEs (except for Ce). This is consistent with findings in the central and intermediate waters of the West Pacific by Behrens et al, (2018a, b). To systematically understand the influence of remineralization on REEs, we summarize the relationship between Nd and AOU in the subsurface and intermediate water (σ_q< 27.5 kg/m^3, depth >DCM), where the remineralization processes are usually pronounced, based on our observations and data from the literature (Behrens et al., 2018a; Behrens et al., 2018b). The results show that Nd increased rapidly as AOU increased in subsurface water (σ_q< 26.6 kg/m^3, depth >DCM) with the relationship yielding about a 4-fold higher slope (0.15±0.06) in the MWR (stations P1-1~P1-4, 37~40°N) vs. south of the MWR (0.04±0.003) (-15~34°N; Figure 5A). However, Nd remained almost constant with increasing AOU in the intermediate water (26.6-27.5 kg/m^3) of the MWR (stations P1-1~P1-4, 37~40°N; Figure 5A). Therefore, in the MWR remineralization processes mainly influenced the REEs in subsurface water, rather than in intermediate water. This may indicate the rapid decomposition of organic matter in the subsurface water, with few organic particles sinking to intermediate water depths in the MWR. Similarly, Nd is positively correlated with nitrate + nitrite in subsurface and intermediate water (σ_q<27.5 kg/m^3, depth >DCM) to the south of the MWR as well as in subsurface water (σ_q< 26.6 kg/m^3, depth >DCM) of the MWR (Figure 5B). This also suggests that the remineralization of sinking organic particles plays a critical role in the production of REEs. We also estimated the addition or removal of Nd in the intermediate water of the MWR (stations P1-1~P1-4, 26.6~27.5 kg/m^3) by using the isopycnal mixing model (section 2.4). The results show that, at 26.6 kg/m^3, the proportion of Nd added to the observed Nd (DNd/Nd) was 21±6%. At 27.5 kg/m^3, there was almost no addition or removal of Nd (DNd/Nd=-6±2%), which is consistent with the above conclusion that remineralization contributes negligible Nd to the intermediate water of the MWR. Overall, our results suggest that the influence of remineralization on REEs varies regionally.

Remineralization processes are related to the ambient environmental context, such as microbial community structure, nutrient supply and exogenous labile organic matter inputs (Church et al., 2000; Carlson et al., 2004; Mills et al., 2008; Carlson et al., 2009; Li et al., 2021). In the MWR, the intrusion front of the Oyashio mainly exists at σ_q < 26.7 kg/m^3 (Zhu et al., 2019), which is almost consistent with the depth (σ_q < 26.6 kg/m^3) where REEs appear to be significantly released by remineralization. The intrusion of the Oyashio into the Kuroshio, with distinct environmental contexts (e.g., temperature, salinity, nutrient supply, and organic matter inputs), may enhance the remineralization in the MWR subsurface water (<26.6 kg/m^3). Enhanced remineralization due to strong mixing is also found in the Luzon Strait near the Kuroshio intrusion (Li et al., 2021). In addition, the regional differences in remineralization might be associated with the plankton community structure. For instance, in the MWR, the phytoplankton are dominated by haptophytes, while in the oligotrophic subtropical region, dinoflagellates are dominant (Suzuki et al., 1997; Lin et al., 2020; Wang et al., 2021; Wang et al., 2022). We suggest that organic detritus from different organisms may have distinct ratios of consumed oxygen and released REEs during the remineralization process. This supposition requires more evidence, such as the ratio of REE concentrations to organic matter in haptophytes vs dinoflagellates. Thus, the water masses mixing and/or the plankton community structure could be responsible for the regional differences of the influence of remineralization on REEs.

Overall, our results emphasize regional differences in the release efficiency of REEs by remineralization. For other trace elements, like iron, the efficiency of organic remineralization is speculated to be one of the reasons for the difference in dissolved iron concentrations between the western and eastern subarctic Pacific (Nishioka et al., 2013). Our results may provide evidence for regional differences in trace elements caused by organic matter remineralization.

4.2 Shelf inputs and lateral transport of REEs

Figure 6 shows the distribution of LREEs (La, Ce, Pr) and La/Yb ratios in surface water (<10 m) in the Northwest Pacific. REE (La, Ce, Pr) concentrations near the margin are higher than those farther away. We suggest that the high REEs in the surface water of the MWR and Oyashio likely originate from the Kuril Islands (Morton et al., 2019). In addition, high La/Yb ratios (>0.35) (Figures 6E and 7A) were observed in northern stations (stations TPS 47 39-1 and SEEDS-II; Piepgras and Jacobsen, 1992; Hara et al., 2009), which reflects the effect of lithogenic material dissolution (Zhang et al., 2008; Pearce et al., 2013). The La/Yb ratio could be the Aleutian Islands signal caught up in the East Kamchatka Current since the elevated La/Yb ratios (0.51±0.51, Supplementary Figure S3A) have been observed in the Aleutian Islands. Furthermore, the high Nd isotopic composition (-2.2 at station CM-S-3 and -2.0 at station TPS 47 39-1) of surface water in the Oyashio also verifies the input of REEs from islands (the Kuril and Aleutian Islands), as volcanic islands usually have more radiogenic Nd (Piepgras and Jacobsen, 1988; Amakawa et al., 2004a, Amakawa et al., 2004b; Fuhr et al., 2021). Therefore, islands are important lithogenic sources of REEs to surface waters of the Northwest Pacific subarctic region and the MWR.

In addition, the Sea of Okhotsk is an important source of materials to the Oyashio and NPIW in the Northwest Pacific, such as Fe (Nishioka et al., 2013), Zn (Kim et al., 2017), Cd (Yang et al., 2018) and anthropogenic CO_2 (Yasuda, 2004). Based on the fact that the Sea of Okhotsk receives a large number of trace elements from rivers and sediments, we believe that Okhotsk seawater may also be an important source of REEs to the Oyashio (Shulkin and Bogdanova, 2003; Nishioka et al., 2007; Nishioka et al., 2013; Nishioka et al., 2014; Kim et al., 2015).

As discussed above, the REEs in the Oyashio Current are sourced from the islands and the Sea of Okhotsk and then supplied to the NPIW in the subtropical region. In the study area, REE concentrations (except for Ce) are mainly influenced by remineralization processes during NPIW transport (see above section 4.1), and their concentration changes vertically, increasing

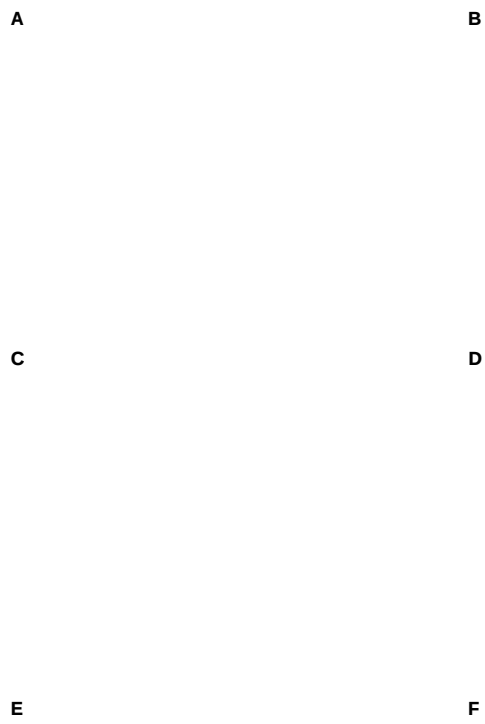

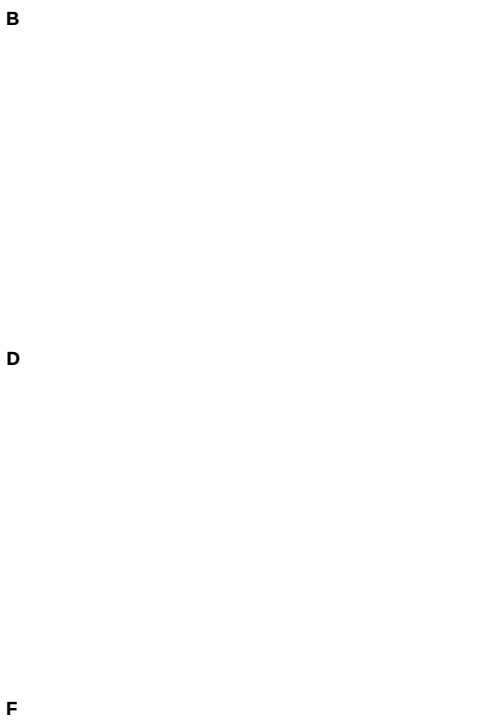

FIGURE 6
Maps showing surface sampling stations. Color bar represents (A) Salinity, (B) La (pmol/kg), (C) Ce (pmol/kg), (D) Pr (pmol/kg), (E) La/Yb and (F) Ce/Ce* (data from this study, Piepgras and Jacobsen (1992); Hara et al. (2009); Behrens et al. (2018a), and Morton et al. (2019)) in surface water (<10 m). The north-south transect is marked with arrows on the map.

with depth (Figures 3D, E, 4B, C). However, unlike other trivalent REEs, dissolved Ce is easily removed by particles in seawater. This is because Ce (III) is easily oxidized to the tetravalent state (Ce(IV)) in seawater and subsequently precipitated as CeO_2 or $Ce(OH)_4$, resulting in the depletion of dissolved Ce and negative Ce anomalies in seawater (Alibo and Nozaki, 1999; Tazoe et al., 2011). Following Morton et al. (2019), in the subarctic region, the Ce concentration was high but Ce/Ce* showed an extremely negative anomaly (<0.2) in surface water (Figures 6C, F), which suggests Ce inputs from the shelf as well as preferential removal of Ce relative to La and Pr by Mn-oxides (Morton et al., 2019). In this study area (transect P1), Ce concentrations were higher at high latitudes than at low latitudes (except for ~1500 m depth at stations P1-7 ~P1-9, Figures 3F): that is, the Ce concentration decreased

FIGURE 7
(A) Distributions of La/Yb with salinity contours in white along the south-north transect shown on the map in Figure 6, and (B) plots of La/Yb versus salinity (data from this study, Piepgras and Jacobsen (1992), and Hara et al. (2009)). La/Yb is significantly negatively correlated with salinity (R^2=0.63, P<0.01).

with distance from the shelf, due to the rapid oxidation and removal of Ce from seawater. At ~1500 m depth at stations P1-7~P1-9, Ce concentrations were slightly higher than in the surrounding seawater (Figure 3F), and the oxygen concentration was the lowest (Figure 3C). This might be explained by fewer oxide particles in the water column or the effect of lateral transport from a low oxygen region, and needs further research. In addition, a strong particulate negative Ce anomaly was observed in the subarctic region (station 2, 155°E, 44°N) by Morton et al. (2019), which may rule out the possibility of supply from an atmospheric source because aerosols generally have no Ce negative anomaly (Morton et al., 2019).

The Oyashio Current acquires the imprints of high La/Yb ratios from the islands through the East Kamchatka Current. As shown in Figure 7A, the highest La/Yb ratios (>0.35) were observed at stations TPS 47 39-1 (Piepgras and Jacobsen, 1992) and SEEDS-II (Hara et al., 2009) (< 100 m) in the East Kamchatka Current. In the low salinity water (<34.25, mainly the Oyashio and NPIW), the high value signature is gradually diluted as the water mass flows southward. It should be noted that because of the lack of REE data in the Sea of Okhotsk, we cannot determine whether the water masses from the Sea of Okhotsk also provided elevated La/Yb ratios to the Oyashio and NPIW. At all stations (≤2000 m), La/Yb is significantly negatively correlated with salinity (R^2=0.63, P<0.01) (Figure 7B). This indicates that the La/Yb ratios are mainly affected by water mass mixing even though it is generally accepted that the particulate process should cause a fractionation of LREEs and HREEs due to their different particle adsorption affinities (Byrne and Kim, 1990; Sholkovitz et al., 1994). Similarly, the Oyashio may also have acquired the signals of Pr/Yb and Nd/Yb ratios from nearby islands (Aleutian and Kamchatka Islands; Figures 8A, B). The islands' Pr/Yb and Nd/Yb signals are more significant than the La/Yb signal (Supplementary Figures S3B, C). NPIW has shown elevated ratios of Pr/Yb and Nd/Yb (Figures 8C, D); however, there is no correlation between Pr/Yb (or Nd/Yb) and salinity (R^2 values were 0.06 and 0.01, respectively). This indicates that La/Yb more faithfully retains the original signature of an end-member than Pr/Yb and Nd/Yb in seawater. This may be related to the fact that La is the only lanthanide element that lacks a 4f electron, resulting in a solution stability that differs from other LREEs in seawater. Otherwise, in seawater, the longer residence time of La compared to other LREEs (Li, 1991; Alibo and Nozaki, 1999; Nozaki, 2001) might also contribute to the water masses tracing values of La/Yb. In summary, the La/Yb ratio provides a useful proxy for studying the flow paths of the Oyashio and NPIW in the North Pacific, and the NPIW is critical for transporting substances that affect marine ecosystems and climate, such as Fe and CO_2 (Yasuda, 2004; Nishioka et al., 2007; Nishioka et al., 2013; Nishioka et al., 2014; Nishioka and Obata, 2017).

REEs ratios have also been used for tracing Southern Ocean water masses (Zhang and Nozaki, 1996; Osborne et al., 2015; Behrens et al., 2018a). For instance, the Ho/Dy ratio may be used to differentiate intermediate/deep water in the Southwest Pacific from Antarctic Bottom Water (Zhang and Nozaki, 1996). The low Dy/Er and high HREE/LREE ratios formed in the East Pacific Rise hydrothermal plume trace the Upper Circumpolar Deep Water

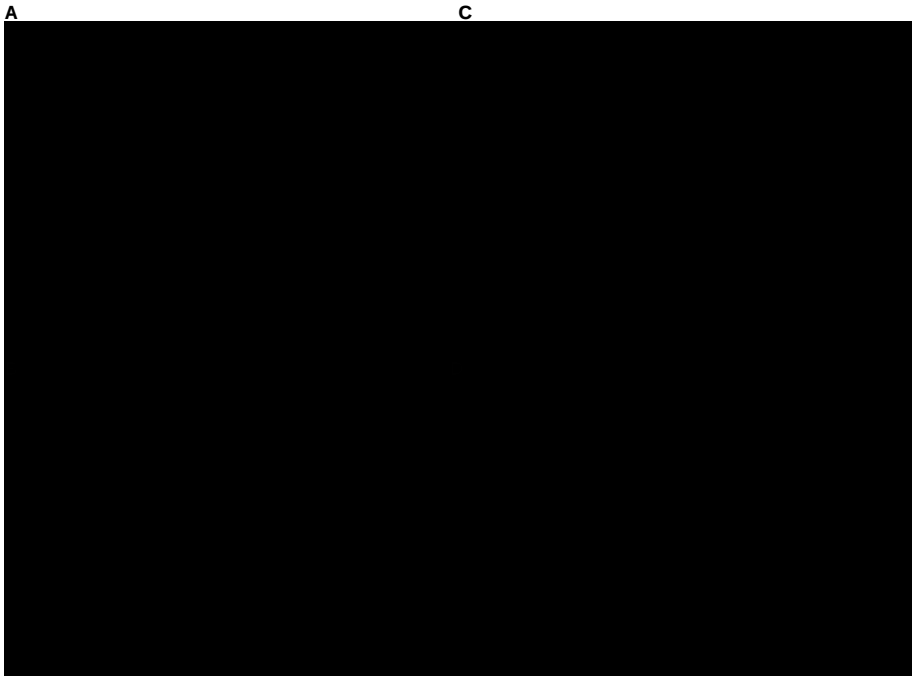

FIGURE 8
Distributions of (A) Pr/Yb ratio and (B) Nd/Yb ratio in the surface water (<10 m). Vertical distributions of (C) Pr/Yb ratio and (D) Nd/Yb ratio with salinity contours in white along the south-north transect (data from this study, Piepgras and Jacobsen (1992); Hara et al. (2009), and Behrens et al. (2018a)).

(Osborne et al., 2015; Behrens et al., 2018a). These examples indicate that the ratios of REEs in the oceans are valuable water mass tracers and should be widely focused on in future studies.

Taken together, lithogenic material input from islands (including the Kuril Islands and the Aleutian Islands) and the Sea of Okhotsk are the important sources of REEs and other trace elements (Fe, Zn, Cd, etc.) to the Oyashio current. It is also an important source for NPIW due to the supply of Oyashio water. The La/Yb ratio is mainly affected by water mass mixing and therefore is a very good tool for tracing the Oyashio and NPIW.

4.3 Estimating cross-shelf Nd fluxes

The marginal seas (including the Sea of Okhotsk, Sea of Japan, East China Sea, South China Sea, and the Bering Sea) may be important REE sources to the Northwest Pacific. We estimated the net Nd fluxes (F_{Nd}^{net}) between the marginal seas and Northwest Pacific based on the following equation:

$$F_{Nd}^{net} = F_w^{inflow} \cdot Nd^m - F_w^{outflow} \cdot Nd^p \quad (8)$$

Where, F_w^{inflow}(or $F_w^{outfolw}$) represents the water flux from the marginal sea to the Northwest Pacific (or from the Northwest Pacific to the marginal sea). Nd^m (or Nd^p) represents the end-member values of Nd concentration in the marginal seas (or the Northwest Pacific). The water fluxes and Nd concentrations are shown in Table 2. The net Nd flux from the Bering Sea was not estimated due to a lack of REE data.

A portion of the East Kamchatka Current flows into the Sea of Okhotsk through the Northern Kuril Islands Strait (mainly in the Kruzenshtern Strait) and then flows out to the Pacific Ocean through the South Kuril Islands Strait (mainly through the Bussol Strait, water depth ~2300 m) (Figure 1; Hill et al., 2003; Shu et al., 2021). Because the water flow flux into the Sea of Okhotsk through the Kruzenshtern Strait is thought to be nearly equal to the outflow flux from the Bussol Strait (Ohshima et al., 2010), we assume that both the inflow and outflow water fluxes are 8.2~8.8 Sv (Katsumata, 2004) (excluding the water exchange caused by tidal processes). Due to the lack of a vertical profile of REEs in the Sea of Okhotsk, the Nd concentration of Okhotsk surface water (Amakawa et al., 2004a) was used to represent the average Nd concentration of the full water column. The net input flux of Nd from the Sea of Okhotsk to the Pacific Ocean was estimated to be 29~32 tNd/y (Table 2 and Figure 9), which is comparable to the input from the Yangtze and Korean rivers combined (20~24 and 7 tNd/y, respectively; Behrens et al., 2018b; Che et al., 2022).

The Tsugaru Strait is the only pathway directly connecting the Sea of Japan and the North Pacific, at a depth of <200 m (Figure 1; Ito et al., 2003). The Tsugaru Warm Current originates from the Sea of Japan and flows into the North Pacific through the Tsugaru Strait with a water flux of 1.1~2.1Sv (Ito et al., 2003). Using above water flux and the weighted average value of Nd in the Sea of Japan (<200 m, Seo and Kim, 2020), we calculated the net Nd input flux to be 159~302 tNd/y (Table 2 and Figure 9). This Nd input flux from the Sea of Japan is of the same order of magnitude as the atmospheric and riverine contributions of Nd to the global oceans (400-630 tNd/

TABLE 2 Estimates of the cross-shelf Nd fluxes from marginal seas.

Marginal Seas	Location	Flow Depth (m)	Flow Magnitude ($10^6 m^3 s^{-1}$)*	Nd (pmol/kg)	Nd Fluxes in straits or channels (t/y)*	Cross-shelf Nd Fluxes from the Marginal Seas to the Northwest Pacific (t/y)*
Sea of Okhotsk	Bussol Strait	Full depth	8.2~8.8[a]	25.6[b#]	953~1023	29~32 (full depth)
	Kruzenshtern Strait	Full depth	-8.2~-8.8[a]	24.82[c%]	-924~-991	
Sea of Japan	Tsugaru Strait	Full depth	1.1~2.1[d]	31.79[e#]	159~302	159~302 (full depth)
East China Sea	Tokara Strait	<200m	13.3~15.3[f]	4.84[g#]	293~336	4~47 (<200m) 142~616 (full depth)
		Full depth	19.9~27.8[f]	13.21[g#]	1194~1668	
	East Taiwan Channel	<200m	-13.8[h]	4.63[i%]	-289	
		Full depth	-22.0[h]	10.55[i%]	-1052	
South China Sea	Luzon Strait	0m~500m	-9~-4.3[j]	7.02[k%]	-287~-137	-298~34 (full depth)**
		500~1500m	1.1~5.0[j]	24.54[k#]	125~557	
		1500m~bottom	-3.4~-2[j]	25.93[k%]	-400~-236	

[a]Katsumata, 2004.
[b]Amakawa et al., 2004a.
[c]Fuhr et al., 2021.
[d]Ito et al., 2003.
[e]Seo and Kim, 2020.
[f]Guo et al., 2013; Liu et al., 2019.
[g]Liu et al., 2022 and our unpublished data.
[h]Johns et al., 2001.
[i]Wu et al., 2015 and unpublished data.
[j]Xu and Oey, 2014 and references therein.
[k]Wu et al., 2015 and unpublished data in the Philippine Sea.
* Positive and negative numbers represent inflow from and outflow to the Northwest Pacific, respectively.
** The Nd fluxes representing the full depth range include results calculated from the water fluxes provided by different literature sources (Xu and Oey, 2014 and references therein), rather than the sum of the maximum and minimum values of Nd fluxes in the three water layers in the table.
[#]End-member values of Nd (pmol/kg) in the marginal seas (Nd^m)
[%] End-member values of Nd (pmol/kg) in the Northwest Pacific (Nd^p).

y and 260-660 tNd/y, respectively ; Greaves et al., 1994; Tachikawa et al., 2003; Arsouze et al., 2009), which are considered important sources of REEs in the oceans (Lacan and Jeandel, 2001; Flierdt et al., 2004; Arsouze et al., 2009).

In the East China Sea, the channels in the Ryukyu Island chain are important links to the Northwest Pacific. The East Taiwan Channel and the Tokara Strait are the main pathways connecting the East China Sea and the Northwest Pacific (Johns et al., 2001; Isobe et al., 2002; Teague et al., 2002; Takikawa et al., 2005; Isobe, 2008). Therefore, we only focus on the fluxes across these two straits. The results show that the net Nd flux from the East China Sea is 142~616 tNd/y, which is relatively large and similar to or greater than the input from the Sea of Japan (159~302 tNd/y, Table 2 and Figure 9). On the other hand, the net Nd input to the Pacific Ocean from the East China Sea shelf at depths of <250 m was estimated to be 113 t/y using Nd isotopes and a box model (Lacan and Jeandel, 2005), which is higher than our result for depths of <200 m (4~47 tNd/y, Table 2). This indicates that our result might be an underestimate, probably due to the fact that we selected a lower average Nd endmember concentration in the Northwest Pacific for our estimation than that used by Lacan and Jeandel (2005).

The water exchange between the Northwest Pacific and the South China Sea occurs mainly through the Luzon Strait. In the Luzon Strait, the surface and deep waters flow from the Pacific to the South China Sea. At intermediate depths, the flow direction is reversed (Chao et al., 1996; Gan et al., 2006; Qu et al., 2006). The Nd fluxes between the Northwest Pacific and the South China Sea at different water layer depths are shown in Table 2. The calculated Nd fluxes for 0-500 m, 500-1500 m, and 1500 m-bottom are -287~-137, 125~557, and -400~-236 t/y (negative values represent input from the Northwest Pacific to the South China Sea), respectively. The net Nd input fluxes for the full water column are -298~34 t/y (Table 2 and Figure 9). This indicates that the South China Sea is a sink of Nd from the Northwest Pacific at 0-500 m and 1500 m-bottom, and a source of Nd in the 500-1500 m water layer. Overall, the South China Sea may be either a net source or a net sink of Nd to the Northwest Pacific depending on the selection of the endmembers in the present estimation. For instance, when the estimated water fluxes at 0-500 m, 500-1500 m, and 1500m-bottom are -9.0, 5.0, and

FIGURE 9
The cross-shelf Nd fluxes (tNd/y) from marginal seas to the Northwest Pacific. Negative values represent input from the Northwest Pacific to the marginal seas.

-2.0 Sv, respectively (Tian et al., 2006), the South China Sea is a source of REEs to the Northwest Pacific with net Nd flux of 34 t/y. When the water fluxes in 0-500 m, 500-1500 m, and 1500 m-bottom are estimated to be -5.1, 2.8, and -3.8 Sv, respectively (Xu and Oey, 2014), the South China Sea is a sink of REEs in the Northwest Pacific with net Nd flux of -298 t/y. It should be noted that there are large uncertainties in the estimated net fluxes of Nd. In particular, the complex water structure (Chen and Wang, 1998; Wang et al., 2010; Zhang et al., 2015) and seasonal variations of water exchange in the Luzon Strait (Xu and Oey, 2014 and references therein) lead to a wide range of water fluxes (Table 2). In addition, there may be seasonal variations in Nd concentrations, which introduce uncertainties in Nd net flux estimates.

In summary, the Sea of Okhotsk, the Sea of Japan and the East China Sea are Nd sources to the Northwest Pacific, with a relatively low net flux of Nd from the Sea of Okhotsk (29~32 t/y) but high fluxes from the Sea of Japan (159~302 t/y) and the East China Sea (142~616 t/y). In contrast, the Nd exchange flux between the South China Sea and the Pacific is subject to water exchange occurring at different water layer depths in the Luzon Strait. The South China Sea is a sink of Nd from the Northwest Pacific at the water layers of 0-500 m (-287~-137 t/y) and 1500m-bottom (-400~-236 t/y), and a source of Nd at 500-1500 m (125~557 t/y), with a net Nd flux range of -298~34 t/y.

5 Conclusions

To study the sources, transport, and biogeochemical cycling of REEs in the Northwest Pacific, we measured dissolved REE concentrations along the P1 transect at 150°E (≤ 2000 m) from 13°N to 40°N. The main findings are as follows:

(1) There are regional differences in the release of REEs by organic matter remineralization. The larger release efficiency of REEs in the MWR (σ_q<26.6 kg/m^3, depth > DCM) compared with that in the subtropical region (σ_q<27.5 kg/m^3, depth > DCM) might be related to stronger water mass mixing and the plankton community structure.

(2) Based on our REE data and previously published trace element data, we suggest that islands in the subarctic region (including the Kuril Islands and Aleutian Islands) and the Sea of Okhotsk are important REE sources to the Northwest Pacific. The La/Yb ratio is a signal of lithogenic dissolution from the Aleutian Islands and can be used as a water mass tracer for the Oyashio Current and NPIW.

(3) The marginal seas usually receive large amounts of REEs, and typically have higher REE concentrations than the open ocean. The estimated net Nd fluxes from the Sea of Okhotsk, Sea of Japan, East China Sea, and the South China Sea were 29~32 t/y, 159~302 t/y, 142~616 t/y, and -298~34 t/y, respectively. Our estimates indicate that the Nd exchange fluxes between the marginal seas and the Northwest Pacific are not negligible.

Overall, our systematic analysis of the source, transport, and biogeochemical cycling of dissolved REEs in the Northwest Pacific provides useful proxy information for tracing regional water masses and estimating cross-shelf REE fluxes. However, the influences of particulate processes (such as the remineralization of organic matter) on REE ratio (e.g., La/Yb) distributions in seawater need further study.

Data availability statement

The original contributions presented in the study are included in the article/Supplementary Material. Further inquiries can be directed to the corresponding authors.

Author contributions

AC: Conceptualization, Investigation, Formal Analysis, Data curation, Writing - original draft. JZ: Conceptualization, Writing-review & editing, Supervision, Project administration. HZ: Data Curation. ZC: Investigation, Data Curation. GC: Formal Analysis, Visualization. ZL: Formal Analysis. YL: Writing – review & editing. QL: Conceptualization, Writing – review & editing, Supervision, Project administration. All authors contributed to the article and approved the submitted version.

Funding

This research was supported by the National Natural Science Foundation of China (Grant 41890801), Fundamental Research Funds for the Central Universities (Grant 202072001), JSPS KAKENHI (Grants JP20H04319, JP22H05206), and Laoshan Laboratory Special Fund of Shandong Province (Grant 2022QNLM010103-1).

Acknowledgments

We thank the captain and crew of the R/V Dongfanghong 3 for their help with sampling. We further thank Wenkai Guan for assisting in the sample collection. Special thanks to Dr. Huijun He for his important guidance during the data analysis. We would like to thank Dr. Richard Smith and Dr. Stella Woodard at Global Aquatic Research LLC for English language editing. We are grateful to Frontiers Science Center for Deep Ocean Multispheres and Earth System, Ocean University of China for providing frozen warehouse space for nutrient sample storage.

Conflict of interest

The authors declare that the research was conducted in the absence of any commercial or financial relationships that could be construed as a potential conflict of interest.

Publisher's note

Supplementary material

The Supplementary Material for this article can be found online at: https://www.frontiersin.org/articles/10.3389/fmars.2023.1135113/full#supplementary-material

SUPPLEMENTARY FIGURE 1
Distributions of (A) the sum of LREEs (pmol/kg) and (B) the sum of HREEs (pmol/kg) along the P1 transect.

SUPPLEMENTARY FIGURE 2
Vertical profiles of (A) the sum of LREEs (pmol/kg) and (B) the sum of HREEs (pmol/kg) with error bars from all stations.

SUPPLEMENTARY FIGURE 3
The ratios of (A) La/Yb, (B) Pr/Yb, and (C) Nd/Yb in rocks from the Aleutian Islands, the Kuril Islands, and Kamchatka Peninsula, including average values and their uncertainties (EarthChem- Access Geochemical Data)

References

Alibo, D. S., and Nozaki, Y. (1999). Rare earth elements in seawater: particle association, shale-normalization, and ce oxidation. Geochim. Cosmochim. Acta 63, 363–372. doi: 10.1016/S0016-7037(98)00279-8

Amakawa, H., Alibo, D. S., and Nozaki, Y. (2004a). Nd Concentration and isotopic composition distributions in surface waters of Northwest pacific ocean and its adjacent seas. Geochem. J. 38, 493–504. doi: 10.2343/geochemj.38.493

Amakawa, H., Nozaki, Y., Alibo, D. S., Zhang, J., Fukugawa, K., and Nagai, H. (2004b). Neodymium isotopic variations in Northwest pacific waters. Geochim. Cosmochim. Acta 68, 715–727. doi: 10.1016/S0016-7037(03)00501-5

Arsouze, T., Dutay, J. C., Lacan, F., and Jeandel, C. (2009). Reconstructing the Nd oceanic cycle using a coupled dynamical – biogeochemical model. Biogeosciences 6, 2829–2846. doi: 10.5194/BG-6-2829-2009

Behrens, M. K., Pahnke, K., Cravatte, S., Marin, F., and Jeandel, C. (2020). Rare earth element input and transport in the near-surface zonal current system of the tropical Western pacific. Earth Planet. Sci. Lett. 549, 116496. doi: 10.1016/j.epsl.2020.116496

Behrens, M. K., Pahnke, K., Paffrath, R., Schnetger, B., and Brumsack, H.-J. (2018a). Rare earth element distributions in the West pacific: Trace element sources and conservative vs. non-conservative behavior. Earth Planet. Sci. Lett. 486, 166–177. doi: 10.1016/j.epsl.2018.01.016

Behrens, M. K., Pahnke, K., Schnetger, B., and Brumsack, H.-J. (2018b). Sources and processes affecting the distribution of dissolved Nd isotopes and concentrations in the West pacific. Geochim. Cosmochim. Acta 222, 508–534. doi: 10.1016/j.gca.2017.11.008

Bertram, C. J., and Elderfield, H. (1993). The geochemical balance of the rare earth elements and neodymium isotopes in the oceans. Geochim. Cosmochim. Acta 57, 1957–1986. doi: 10.1016/0016-7037(93)90087-D

Bryan, J. R., Rlley, J. P., and Williams, P. L. (1976). A winkler procedure for making precise measurements of oxygen concentration for productivity and related studies. J.Exp. Mar. Biol. Ecol. 21 (3), 191–197. doi: 10.1016/0022-0981(76)90114-3

Byrne, R. H., and Kim, K.-H. (1990). Rare earth element scavenging in seawater. Geochim. Cosmochim. Acta 54, 2645–2656. doi: 10.1016/0016-7037(90)90002-3

Carlson, C. A., Giovannoni, S. J., Hansell, D. A., Goldberg, S. J., Parsons, R., and Vergin, K. (2004). Interactions among dissolved organic carbon, microbial processes, and community structure in the mesopelagic zone of the northwestern Sargasso Sea. Limnol. Oceanogr. 49 (4), 1073–1083. doi: 10.4319/lo.2004.49.4.1073

Carlson, C. A., Morris, R., Parsons, R., Treusch, A. H., Giovannoni, S. J., and Vergin, K. (2009). Seasonal dynamics of SAR11 populations in the euphotic and mesopelagic zones of the northwestern Sargasso Sea. ISME J. 3 (3), 283–295. doi: 10.1038/ismej.2008.117

Chao, S. Y., Shaw, P. T., and Wu, S. Y. (1996). Deep water ventilation in the south China Sea. Deep Sea Res. Part I Oceanogr. Res. Pap. 43, 445–466. doi: 10.1016/0967-0637(96)00025-8

Che, H., Zhang, J., Liu, Q., He, H., and Zhao, Z.-Q. (2022). Refining the contribution of riverine particulate release to the global marine Nd budget. Prog. Earth Planet Sci. 9, 22. doi: 10.1186/s40645-022-00479-2

Chen, C. T. A., and Wang, S. L. (1998). Influence of intermediate water in the western Okinawa trough by the outflow from the south China Sea. J. Geophys. Res. 103, 12683–12688. doi: 10.1029/98JC00366

Church, M. J., Hutchins, D. A., and Ducklow, H. W. (2000). Limitation of bacterial growth by dissolved organic matter and iron in the southern ocean. Appl. Environ. Microbiol. 66 (2), 455–466. doi: 10.1128/AEM.66.2.455-466.2000

de Baar, H. J. W., Bacon, M. P., Brewer, P. G., and Bruland, K. W. (1985). Rare earth elements in the pacific and Atlantic oceans. Geochim. Cosmochim. Acta 49, 1943–1959. doi: 10.1016/0016-7037(85)90089-4

de Baar, H. J. W., Bruland, K. W., Schijf, J., van Heuven, S. M. A. C., and Behrens, M. K. (2018). Low cerium among the dissolved rare earth elements in the central north pacific ocean. Geochim. Cosmochim. Acta 2365-, 40. doi: 10.1016/j.gca.2018.03.003

Du, C., Liu, Z., Dai, M., Kao, S. J., Cao, Z., Zhang, Y., et al. (2013). Impact of the kuroshio intrusion on the nutrient inventory in the upper northern south China Sea: Insights from an isopycnal mixing model. Biogeosciences 10 (10), 6419–6432. doi: 10.5194/bg-10-6419-2013

Elderfield, H. (1988). The oceanic chemistry of the rare-earth elements. Phil. Trans. R. Soc Lond. A 325, 105–126. doi: 10.1098/rsta.1988.0046

Elderfield, H., and Greaves, M. J. (1982). The rare earth elements in seawater. Nature 296, 214–219. doi: 10.1038/296214a0

Flierdt, T., Frank, M., Lee, D.-C., Halliday, A. N., Reynolds, B. C., and Hein, J. R. (2004). New constraints on the sources and behavior of neodymium and hafnium in seawater from pacific ocean ferromanganese crusts. Geochim. Cosmochim. Acta 68, 3827–3843. doi: 10.1016/j.gca.2004.03.009

Frij̈e, H., Pahnke, K., Schnetger, B., Brumsack, H. J., Dulai, H., and Fitzsimmons, J. N. (2016). Hawaiian Imprint on dissolved Nd and Ra isotopes and rare earth elements in the central north pacific: Local survey and seasonal variability. Geochim. Cosmochim. Acta 189, 110–131. doi: 10.1016/j.gca.2016.06.001

Fuhr, M., Laukert, G., Yu, Y., Nöthberg, D., and Frank, M. (2021). Tracing water mass mixing from the equatorial to the north pacific ocean with dissolved neodymium isotopes and concentrations. Front. Mar. Sci. 7. doi: 10.3389/fmars.2020.603761

Gan, J., Li, H., Curchitser, E. N., and Haidvogel, D. B. (2006). Modeling south China Sea circulation: Response to seasonal forcing regimes. J. Geophys. Res. 111, C06034. doi: 10.1029/2005JC003298

Garcia-Solsona, E., Pena, L. D., Paredes, E., Pérez-Asensio, J. N., Quirós-Collazos, L., Lirer, F., et al. (2020). Rare earth elements and Nd isotopes as tracers of modern ocean circulation in the central Mediterranean Sea. Prog. Oceanogr. 185, 102340. doi: 10.1016/j.pocean.2020.102340

Greaves, M. J., Statham, P. J., and Elderfield, H. (1994). Rare earth element mobilization from marine atmospheric dust into seawater. Mar. Chem. 46, 255–260. doi: 10.1016/0304-4203(94)90081-7

Guo, X. Y., Zhu, X.-H., Long, Y., and Huang, D. J. (2013). Spatial variations in the kuroshio nutrient transport from the East China Sea to south of Japan. Biogeosciences 10, 6403–6417. doi: 10.5194/bg-10-6403-2013

Hara, Y., Obata, H., Doi, T., Hongo, Y., Gamo, T., Takeda, S., et al. (2009). Rare earth elements in seawater during an iron-induced phytoplankton bloom of the western subarctic pacific (SEEDS-II). Deep Sea Res. Part II Top. Stud. Oceanogr. 56, 2839–2851. doi: 10.1016/j.dsr2.2009.06.009

Hatje, V., Bruland, K. W., and Flegal, A. R. (2014). Determination of rare earth elements after pre-concentration using NOBIAS-chelate PA-1® resin: Method development and application in the San Francisco bay plume. Mar. Chem. 160, 34–41. doi: 10.1016/j.marchem.2014.01.006

Hatta, M., and Zhang, J. (2006). Possible source of advected water mass and residence times in the multi-structured Sea of Japan using rare earth elements. Geophys. Res. Lett. 33, L16606. doi: 10.1029/2006GL026537

Hill, K. L., Weaver, A. J., Freeland, H. J., and Bychkov, A. (2003). Evidence of change in the sea of Okhotsk: Implications for the north pacific. Atmos. -Ocean 41, 49–63. doi: 10.3137/ao.410104

Hu, D., Wu, L., Cai, W., Gupta, A. S., Ganachaud, A., Qiu, B., et al. (2015). Pacific western boundary currents and their roles in climate. Nature 522 (7556), 299–308. doi: 10.1038/nature14504

Isobe, A. (2008). Recent advances in ocean-circulation research on the yellow Sea and East China Sea shelves. J. Phys. Oceanogr. 64 (4), 569–584. doi: 10.1007/s10872-008-0048-7

Isobe, A., Ando, M., Watanabe, T., Senjyu, T., Sugihara, S., and Manda, A. (2002). Freshwater and temperature transports through the tsushima-Korea straits. J. Geophys. Res. 107 (7), 2-1–2-20. doi: 10.1029/2000JC000702

Ito, T., Togawa, O., Ohnishi, M., Isoda, Y., Nakayama, T., Shima, S., et al. (2003). Variation of velocity and volume transport of the tsugaru warm current in the winter of 1999-2000. Geophys. Res. Lett. 30(13), 11-1-11-4. doi: 10.1029/2003GL017522

Johannesson, K. H., and Burdige, D. J. (2007). Balancing the global oceanic neodymium budget: Evaluating the role of groundwater. Earth Planet. Sci. Lett. 253, 129–142. doi: 10.1016/j.epsl.2006.10.021

Johns, W. E., Lee, T. N., Zhang, D., Zantopp, R., Liu, C.-T., and Yang, Y. (2001). The kuroshio East of Taiwan: Moored transport observations from the WOCE PCM-1 array. J. Phys. Oceanogr. 31, 1031–1053. doi: 10.1175/1520-0485(2001)031<1031:TKEOTM>2.0.CO;2

Katsumata, K. (2004). Water exchange and tidal currents through the bussol' strait revealed by direct current measurements. J. Geophys. Res. 109, C09S06. doi: 10.1029/2003JC001864

Kim, T., Obata, H., Kondo, Y., Ogawa, H., and Gamo, T. (2015). Distribution and speciation of dissolved zinc in the western north pacific and its adjacent seas. Mar. Chem. 173, 330–341. doi: 10.1016/j.marchem.2014.10.016

Kim, T., Obata, H., Nishioka, J., and Gamo, T. (2017). Distribution of dissolved zinc in the Western and central subarctic north pacific: Zinc in the subarctic north pacific. Global Biogeochem. Cycles 31, 1454–1468. doi: 10.1002/2017GB005711

Lacan, F., and Jeandel, C. (2001). Tracing Papua new Guinea imprint on the central equatorial pacific ocean using neodymium isotopic compositions and rare earth element patterns. Earth Planet. Sci. Lett. 186, 497–512. doi: 10.1016/S0012-821X(01)00263-1

Lacan, F., and Jeandel, C. (2005). Neodymium isotopes as a new tool for quantifying exchange fluxes at the continent–ocean interface. Earth Planet. Sci. Lett. 232, 245–257. doi: 10.1016/j.epsl.2005.01.004

Lambelet, M., van de Flierdt, T., Crocket, K., Rehkämper, M., Kreissig, K., Coles, B., et al. (2016). Neodymium isotopic composition and concentration in the western north Atlantic ocean: Results from the GEOTRACES GA02 section. Geochim. Cosmochim. Acta 177, 1–29. doi: 10.1016/j.gca.2015.12.019

Li, Y. H. (1991). Distribution patterns of the elements in the ocean: A synthesis. Geochim. Cosmochim. Acta 55 (11), 3223–3240. doi: 10.1016/0016-7037(91)90485-N

Li, X., Liang, H., Zhuang, G., Wu, Y., Li, S., Zhang, H., et al. (2022). Annual variations of isoprene and other non-methane hydrocarbons in the jiaozhou bay on the East coast of north China. JGR Biogeosciences 127. doi: 10.1029/2021JG006531

Li, X., Wu, K., Gu, S., Jiang, P., Li, H., Liu, Z., et al. (2021). Enhanced biodegradation of dissolved organic carbon in the western boundary kuroshio current when intruded to the marginal south China Sea. JGR Oceans 126. doi: 10.1029/2021JC017585

Lin, G., Chen, Y., Huang, J., Wang, Y., Ye, Y., and Yang, Q. (2020). Regional disparities of phytoplankton in relation to different water masses in the Northwest pacific ocean during the spring and summer of 2017. Acta Oceanol. Sin. 39, 107–118. doi: 10.1007/s13131-019-1511-6

Liu, Z., Nakamura, H., Zhu, X., Nishina, A., Guo, X., and Dong, M. (2019). Tempo-spatial variations of the kuroshio current in the tokara strait based on long-term ferryboat ADCP data. J. Geophys. Res. Oceans 124, 6030–6049. doi: 10.1029/2018JC014771

Liu, Q., Zhang, J., He, H., Ma, L., Li, H., Zhu, S., et al. (2022). Significance of nutrients in oxygen-depleted bottom waters via various origins on the mid-outer shelf of the East China Sea during summer. Sci. Total Environ. 826, 154083. doi: 10.1016/j.scitotenv.2022.154083

Mills, M. M., Moore, C. M., Langlois, R., Milne, A., Achterberg, E., Nachtigall, K., et al. (2008). Nitrogen and phosphorus co-limitation of bacterial productivity and growth in the oligotrophic subtropical north Atlantic. Limnol. Oceanogr. 53 (2), 824–834. doi: 10.4319/lo.2008.53.2.0824

Morton, P. L., Landing, W. M., Shiller, A. M., Moody, A., Kelly, T. D., Bizimis, M., et al. (2019). Shelf inputs and lateral transport of Mn, Co, and ce in the Western north pacific ocean. Front. Mar. Sci. 6. doi: 10.3389/fmars.2019.00591

Nishioka, J., Mitsudera, H., Yasuda, I., Liu, H., Nakatsuka, T., and Volkov, Y. N. (2014). Biogeochemical and physical processes in the Sea of Okhotsk and the linkage to the pacific ocean. Prog. Oceanogr. 126, 1–27. doi: 10.1016/j.pocean.2014.04.027

Nishioka, J., Nakatsuka, T., Watanabe, Y. W., Yasuda, I., Kuma, K., Ogawa, H., et al. (2013). Intensive mixing along an island chain controls oceanic biogeochemical cycles. Global Biogeochem. Cycles. 27, 920–929. doi: 10.1002/gbc.20088

Nishioka, J., and Obata, H. (2017). Dissolved iron distribution in the western and central subarctic pacific: HNLC water formation and biogeochemical processes: Dissolved fe distribution in the western and central subarctic pacific. Limnol. Oceanogr. 62, 2004–2022. doi: 10.1002/lno.10548

Nishioka, J., Ono, T., Saito, H., Nakatsuka, T., Takeda, S., Yoshimura, T., et al. (2007). Iron supply to the western subarctic pacific: Importance of iron export from the Sea of Okhotsk. J. Geophys. Res. 112, C10012. doi: 10.1029/2006JC004055

Nitani, H. (1972). "Beginning of the kuroshio," in Kuroshio, physical aspect of the Japan current. Eds. H. Stommel and K. Yoshida (Tokyo, Japan: University of Tokyo Press), 129–163.

Nozaki, Y. (2001). "Rare earth elements and their isotopes in the ocean," in Encyclopedia of ocean sciences (New York: Elsevier), 2354–2366. doi: 10.1006/rwos.2001.0284

Ohshima, K. I., Nakanowatari, T., Riser, S., and Wakatsuchi, M. (2010). Seasonal variation in the in- and outflow of the Okhotsk Sea with the north pacific. Deep Sea Res. Part II Top. Stud. Oceanogr. 57, 1247–1256. doi: 10.1016/j.dsr2.2009.12.012

Osborne, A. H., Haley, B. A., Hathorne, E. C., Plancherel, Y., and Frank, M. (2015). Rare earth element distribution in Caribbean seawater: Continental inputs versus lateral transport of distinct REE compositions in subsurface water masses. Mar. Chem. 177, 172–183. doi: 10.1016/j.marchem.2015.03.013

Parsons, T. R., Maita, Y., and Lalli, C. M. (1984). A manual of chemical and biological methods for seawater analysis (New York: Pergamon Press, 99-112).

Pearce, C. R., Jones, M. T., Oelkers, E. H., Pradoux, C., and Jeandel, C. (2013). The effect of particulate dissolution on the neodymium (Nd) isotope and rare earth element (REE) composition of seawater. Earth Planet. Sci. Lett. 369-370, 138–147. doi: 10.1016/j.epsl.2013.03.023

Persson, P.-O., Andersson, P. S., Zhang, J., and Porcelli, D. (2011). Determination of Nd isotopes in water: A chemical separation technique for extracting Nd from seawater using a chelating resin. Anal. Chem. 83, 1336–1341. doi: 10.1021/ac102559k

Piepgras, D. J., and Jacobsen, S. B. (1988). The isotopic composition of neodymium in the north pacific. Geochim. Cosmochim. Acta 52869, 1373–1381. doi: 10.1016/0016-7037(88)90208-6

Piepgras, D. J., and Jacobsen, S. B. (1992). The behavior of rare earth elements in seawater: Precise determination of variations in the north pacific water column. Geochim. Cosmochim. Acta 56 (5), 1851–1861. doi: 10.1016/0016-7037(92)90315-A

Qiu, B. O., and Chen, S. (2011). Effect of decadal kuroshio extension jet and eddy variability on the modification of north pacific intermediate water. J. Phys. Oceanogr. 41 (3), 503–515. doi: 10.1175/2010JPO4575.1

Qu, T., Girton, J. B., and Whitehead, J. A. (2006). Deepwater overflow through Luzon strait. J. Geophys. Res. 111, C01002. doi: 10.1029/2005JC003139

Rogachev, K. A., Carmack, E. C., and Salomatin, A. S. (2000). Recent thermohaline transition in the pacific western subarctic boundary currents and their fresh core eddies: The response of sound-scattering layers. J. Mar. Syst. 26 (3), 239–258. doi: 10.1016/S0924-7963(00)00036-1

Schlitzer, R. (2015) Ocean data view. Available at: http://odv.awi.de.

Seo, H., and Kim, G. (2020). Rare earth elements in the East Sea (Japan sea): Distributions, behaviors, and applications. Geochim. Cosmochim. Acta 286, 19–28. doi: 10.1016/j.gca.2020.07.016

Sholkovitz, E. R., Landing, W. M., and Lewis, B. L. (1994). Ocean particle chemistry: The fractionation of rare earth elements between suspended particles and seawater. Geochim. Cosmochim. Acta 58, 1567–1579. doi: 10.1016/0016-7037(94)90559-2

Shu, H. W., Mitsudera, H., Yamazaki, K., Nakamura, T., Kawasaki, T., Nakanowatari, T., et al. (2021). Tidally modified western boundary current drives interbasin exchange between the Sea of Okhotsk and the north pacific. Sci. Rep. 11, 12037. doi: 10.1038/s41598-021-91412-y

Shulkin, V. M., and Bogdanova, N. N. (2003). Mobilization of metals from riverine suspended matter in seawater. Mar. Chem. 83, 157–167. doi: 10.1016/S0304-4203(03)00109-9

Stichel, T., Hartman, A. E., Duggan, B., Goldstein, S. L., Scher, H., and Pahnke, K. (2015). Separating biogeochemical cycling of neodymium from water mass mixing in the Eastern north Atlantic. Earth Planet. Sci. Lett. 412, 245–260. doi: 10.1016/j.epsl.2014.12.008

Suga, T., Kato, A., and Hanawa, K. (2000). North pacific tropical water: its climatology and temporal changes associated with the climate regime shift in the 1970s. Prog. Oceanogr. 47, 223–256. doi: 10.1016/S0079-6611(00)00037-9

Suzuki, K., Handa, N., Kiyosawa, H., and Ishizaka, J. (1997). Temporal and spatial distribution of phytoplankton pigments in the central pacific ocean along 175°E during the Boreal summers of 1992 and 1993. J. Oceanogr. 53, 383–396.

Tachikawa, K., Athias, V., and Jeandel, C. (2003). Neodymium budget in the modern ocean and paleo-oceanographic implications. J. Geophys. Res. 108, 10-1-10-13. doi: 10.1029/1999JC000285

Takata, H., Tagami, K., Aono, T., and Uchida, S. (2009). Determination of trace levels of yttrium and rare earth elements in estuarine and coastal waters by inductively coupled plasma mass spectrometry following preconcentration with NOBIAS-CHELATE resin. Atomic Spectrosc. 30, 10–19.

Takikawa, T., Yoon, J. H., and Cho, K. D. (2005). The tsushima warm current through tsushima straits estimated from ferryboat ADCP data. J. Phys. Oceanogr 35 (6), 1154–1168. doi: 10.1175/JPO2742.1

Talley, L. D., Nagata, Y., Fujimura, M., Iwao, T., Kono, T., Inagake, D., et al. (1995). North pacific intermediate water in the Kuroshio/Oyashio mixed water region. J. Phys. Oceanogr. 25, 475–501. doi: 10.1175/1520-0485(1995)025<0475:NPIWIT>2.0.CO;2

Taylor, S. R., and McLennan, S. M. (1985). The continental crust, its composition and evolution: An examination of the geochemical record preserved in sedimentary rocks (Oxford: Blackwell Scientific).

Tazoe, H., Obata, H., and Gamo, T. (2011). Coupled isotopic systematics of surface cerium and neodymium in the pacific ocean. Geochem. Geophys. Geosyst. 12, Q04004. doi: 10.1029/2010GC003342

Teague, W. J., Jacobs, G. A., Perkins, H. T., Book, J. W., Chang, K. I., and Suk, M. S. (2002). Low-frequency current observations in the Korea/Tsushima strait. J. Phys. Oceanogr. 32, 1621–1641. doi: 10.1175/1520-0485(2002)032<1621:LFCOIT>2.0.CO;2

Tian, J., Yang, Q., Liang, X., Xie, L., Hu, D., Wang, F., et al. (2006). Observation of Luzon strait transport. Geophys. Res. Lett. 33, L19607. doi: 10.1029/2006GL026272

Wang, Y., Bi, R., Zhang, J., Gao, J., Takeda, S., Kondo, Y., et al. (2022). Phytoplankton distributions in the kuroshio-oyashio region of the Northwest pacific ocean: Implications for marine ecology and carbon cycle. Front. Mar. Sci. 9. doi: 10.3389/fmars.2022.865142

Wang, Y., Kang, J., Sun, X., Huang, J., Lin, Y., and Xiang, P. (2021). Spatial patterns of phytoplankton community and biomass along the kuroshio extension and adjacent waters in late spring. Mar. Biol. 168, 40. doi: 10.1007/s00227-021-03846-7

Wang, Z., Yuan, D. L., and Hou, Y. J. (2010). Effect of meridional wind on gap-leaping western boundary current. Chin. J. Oceanol. Limnol. 28 (2), 354–358. doi: 10.1007/s00343-010-9281-1

Wu, Q., Colin, C., Liu, Z., Douville, E., Dubois-Dauphin, Q., and Frank, N. (2015). New insights into hydrological exchange between the south China Sea and the Western pacific ocean based on the Nd isotopic composition of seawater. Deep Sea res. part II. Top. Stud. Oceanogr. 122, 25–40. doi: 10.1016/j.dsr2.2015.11.005

Xu, F. H., and Oey, L. Y. (2014). State analysis using the local ensemble transform kalman filter (LETKF) and the three-layer circulation structure of the Luzon strait and the south China Sea. Ocean Dyn. 64, 905–923. doi: 10.1007/s10236-014-0720-y

Yang, S. C., Zhang, J., Sohrin, Y., and Ho, T. Y. (2018). Cadmium cycling in the water column of the kuroshio-oyashio extension region: Insights from dissolved and particulate isotopic composition. Geochim. Cosmochim. Acta 233, 66–80. doi: 10.1016/j.gca.2018.05.001

Yasuda, I. (2004). North pacific intermediate water: Progress in sage (subarctic gyre experiment) and related projects. J. Phys. Oceanogr. 60 (2), 385–395. doi: 10.1023/B:JOCE.0000038344.25081.42

Yasuda, I., Hiroe, Y., Komatsu, K., Kawasaki, K., Joyce, T. M., Bahr, F., et al. (2001). Hydrographic structure and transport of the oyashio south of Hokkaido and the formation of north pacific intermediate water. J. Geophys. Res. 106, 6931–6942. doi: 10.1029/1999JC000154

Yasuda, I., Okuda, K., and Shimizu, Y. (1996). Distribution and modification of north pacific intermediate water in the kuroshio-oyashio interfrontal zone. J. Phys. Oceanogr. 26, 448–465. doi: 10.1175/1520-0485(1996)026<0448:DAMONP>2.0.CO;2

Zhang, Y., Lacan, F., and Jeandel, C. (2008). Dissolved rare earth elements tracing lithogenic inputs over the kerguelen plateau (Southern ocean). Deep Sea Res. Part II: Topical Stud. Oceanography 55, 638–652. doi: 10.1016/j.dsr2.2007.12.029

Zhang, J., Liu, Q., Bai, L., and Matsuno, T. (2018). Water mass analysis and contribution estimation using heavy rare earth elements: Significance of kuroshio intermediate water to central East China Sea shelf water. Mar. Chem. 204, 172–180. doi: 10.1016/j.marchem.2018.07.011

Zhang, J., and Nozaki, Y. (1996). Rare earth elements and yttrium in seawater: ICP-MS determinations in the East Caroline, coral Sea, and south Fiji basins of the western south pacific ocean. Geochim. Cosmochim. Acta 60, 4631–4644. doi: 10.1016/S0016-7037(96)00276-1

Zhang, J., and Nozaki, Y. (1998). Behavior of rare earth elements in seawater at the ocean margin: a study along the slopes of the sagami and nankai troughs near Japan. Geochim. Cosmochim. Acta 62, 1307–1317. doi: 10.1016/S0016-7037(98)00073-8

Zhang, Z., Zhao, W., Tian, J., Yang, Q., and Qu, T. (2015). Spatial structure and temporal variability of the zonal flow in the Luzon strait. J. Geophys. Res. Oceans 120, 759–776. doi: 10.1002/2014JC010308

Zheng, X. Y., Plancherel, Y., Saito, M. A., and Scott, P. M. (2016). And Henderson, G Rare earth elements (REEs) in the tropical south Atlantic and quantitative deconvolution of their non-conservative behavior. M.Geochim. Cosmochim. Acta 177, 217–237. doi: 10.1016/j.gca.2016.01.018

Zhu, K. L., Chen, X., Mao, K. F., Hu, D., Hong, S., and Li, Y. (2019). Mixing characteristics of the subarctic front in the kuroshio-oyashio confluence region. Oceanologia 61, 103–113. doi: 10.1016/j.oceano.2018.07.004